

## Automated Defect Detection for Epoxy-Carbon Prepreg Laminates in Data Fusion Approach

by P. Zhu\*, Z. Wei\* \*\*\* \*\*\*\*, O. Zahra\*, G. Marchais\*, P. Servais\*\* , T. Boulanger \*\*\*\*\*

and X. Maldague\*

\* Université Laval, 2325 Rue de l'université, QC G1V, Québec, Canada,

\*\* MPP, Aero & Industrial Solutions 1er avenue 66 – B-4040 Herstal, Belgium

\*\*\* University of Applied Sciences in Saarbrücken, 66117 Saarbrücken, Germany

\*\*\*\* Fraunhofer Institute for Nondestructive Testing IZFP, 66123 Saarbrücken, Germany

\*\*\*\*\* Optrion SA, Avenue du Pré-Aily 25, Parc Scientifique du Sart-Tilman, 4031 Liège, Belgium

### Abstract

Fibre-reinforced polymer composites have become widely used materials in the manufacturing of aerospace, boat building, and automotive, due to their high specific stiffness and strength, chemical resistance, etc. However, the curing process has a major influence on void content and fibre-matrix interface, affecting the quality of the composite part. In this work, non-destructive testing based on infrared thermography and shearography is used to detect the subsurface defects and impact damage in epoxy-carbon prepreg laminates. Different data fusion methods are used for the incrementing of the detection ability. For the requirement of industrial applications, an automated defect detection method named YOLOv7 is performed in the data fusion view. To improve the detection ability of YOLOv7, a data augmentation method named MixUp is used to construct the datasets obtained from the simulation. The experimental results show the excellent detection capacity of the proposed method. Furthermore, the experimental results also illustrate that the data fusion technique of the Dempster-Shafer method has the best effect compared with the other methods.

### 1. Introduction

Fibre-reinforced polymer composites have been increasingly used in the manufacturing of lightweight constructions, including aerospace, boat building, and automotive, due to their high specific stiffness and strength, chemical resistance, and thermo-mechanical properties [1]. Carbon fibre prepreps impregnated with epoxy resins have especially been the material of choice for the primary structural composite parts. They are typically cured in an autoclave where the application of high temperature, vacuum, pressure, heat-up rate and cure temperature are controlled. However, the curing process has a major influence on void content and fibre-matrix interface, affecting the quality of the composite part.

Currently, there are few inspection methods for epoxy-carbon prepreps. Non-destructive testing (NDT) is considered a means of identifying defects in the curing process. Among NDT techniques, optical excitation thermography (OET) and shearography, as two optical image diagnosis techniques, are increasingly and particularly attractive [2-6]. In OET, the sample is subjected to an external heat source to create a temperature contrast. The defects can be detected by analyzing the temperature difference. In shearography, when the sample is subjected to an external heat source, the defects in the sample will generate deformation different from the surroundings and forms a distinct deformation gradient, which is mainly illustrated as a butterfly speckle interferogram in a shearography image. Scientific measurements based on a single sensor can provide only limited information about the environment in which it operates [7-10]. However, information from different NDT systems can be conflicting, incomplete, or vague if looked at as discrete data. The concept of data fusion can be used to combine information from multiple NDT systems and help in decision-making to reduce human error interpretation.

Multiple heuristic and analytical techniques for data fusion have appeared in literature during the last 20 years. For instance, classical data fusion techniques including the average method, difference method, weighted average method and Hadamard method were used [11]. However, there was no optimal combination technique from the literature, and all these data fusion techniques varied from one application to another. To solve this problem, methods based on Bayesian probabilistic reasoning and the Dempster-Shafer theory of evidence had been proposed [12-14]. Furthermore, a novel unified and unsupervised end-to-end image fusion network, termed as U2Fusion, has been proposed recently, which can solve different fusion problems, including multi-modal, multi-exposure, and multi-focus cases [15].

The data fusion techniques at pixel level may be adequate to increase knowledge about defect location and characterization and to reduce ambiguity. However, for different and complex defective features, it is difficult to distinguish defective areas and non-defective areas such as the combination of optical excitation thermography and shearography. In OET, the defective area and non-defective area can be easily distinguished by the temperature difference. Generally, the area with a high temperature (pixel value) denotes defective areas, and the area with a low temperature (pixel value)



denotes non-defective areas. In shearography, the defect feature is complicated. The defective area looks like a butterfly speckle interferogram. It means that both high pixel value and low pixel denote defective area, and the middle pixel value denotes non-defective area. It is possible to imagine that the fusion results will generate a lot of noise. Therefore, developing an automatic defect detection technique in the data fusion view is significant.

In this work, the epoxy-carbon prepreg laminates with impact damage and inserts were detected by infrared thermography technique and shearography technique. The principal component analysis was used to increase the image contrast and reduce the noise. Then, different data fusion techniques were applied to the processed images. To identify the defects, YOLOv7, the latest detector architecture with fast detection speed and high precision, is adopted to evaluate different data fusion results. The datasets for training were generated by simulation. A data augmentation method named MixUp is used to improve the detection ability of the network. The experimental results show the great performance of the automated defects detection methods in the data fusion view.

## 2. Theory and method

Data fusion models differ from author to author, but they all agree on a three-level process: the signal level, the level of evidence and the level of dynamics. The integration phase at the signal level is called data fusion. At the level of evidence, it is referred to as features fusion, and decision fusion relates to the level of dynamics. In this work, what the authors study is focused on the signal level and the level of dynamics. In addition, a deep learning network was applied to evaluate different data fusion techniques.

### 2.1. Data fusion methods

In this section, several commonly used data fusion techniques are introduced and applied for two different sensors, including shearography and infrared thermography. A combination of basic and information theory-based fusion algorithms have been selected: average to indicate the equal performance of the sources, the difference to clarify contradiction between sources, weighted average to highlight the importance of one source over the other, and Hadamard to increase the signal-to-noise ratio, as shown in Table 1.

**Table 1.** Data fusion algorithms with description and mathematical formulas

Fusion algorithm	Description	Mathematical formula
Average	The average from two sources: SH <sup>1</sup> and IR <sup>2</sup>	(SH+IR)/2
Difference	Differentiating one matrix (IR) from the other (SH)	SH-IR
Weighted average	Weighted average when one matrix has four times higher weight than the other	(5*SH+IR)/6 (SH+5*IR)/6
Hadamard product	Pixel-wise multiplication of same-size matrices	SH.*IR

<sup>1</sup>SH denotes the feature matrix of shearography. <sup>2</sup>IR denotes the feature matrix of infrared thermography.

These four basic fusion algorithms include average, difference, weight difference and Hadamard product. The average algorithm has been implemented by the average of each feature matrices. The difference algorithm has been implemented by the difference of two feature matrices when two sensors are inversely correlated. Two different weighted average algorithms have been applied where the weighted average of the shearography feature matrix is four times higher (or lower) than that of the infrared thermography feature matrix. In addition, the Hadamard product is an algebraic operation based on pixel-wise multiplication of same-size matrices.

Bayesian analysis was carried out by combining conditional and priori information from both techniques. At the heart of Bayesian data fusion is the idea of representing uncertainty using probability distributions. The Bayesian theory is adapted for decision making. The details that applying the Bayesian theory in data fusion are as follows. The first step is to resize the images from different sensors. The second step is to calculate the Gaussian mixture model and the posteriori probability based on pixel values. The last step is to calculate the fusion pixel values based on Bayesian formula.

The Dempster – Shafer theory is often described as an extension of the probability theory or a generalization of the Bayesian inference method. The details that applying the Dempster-Shafer theory in data fusion are as follows. The first step is to resize the images from different sensors. The second step is to calculate the probability density function of each pixel value. The last step is to calculate the fusion pixel values based on Dempster-Shafer formula.

Scientific measurements using identical or disparate multiple sensors generate large amounts of data of similar or different classes which need to be processed in a meaningful way. The systematic integration of multisensory information is known as data fusion. In this work, the unsupervised neural network named U2Fusion was used to combine the IR image and visual image. The details about the structure of U2Fusion can be shown in the reference paper [15].

## 2.2. Automatic defect detection

As mentioned before, there are many data fusion techniques including classical methods and neural networks. It is hard to evaluate the advantages and disadvantages among different methods. In this work, YOLOv7, a latest detector architecture with fast detection speed and high precision, is adopted to evaluate different data fusion results [16]. The YOLOv7 network consists of three parts, including Backbone, feature pyramid network (FPN) and YOLO Head. Backbone is the backbone feature extraction network of YOLOv7. The input images are first extracted in the backbone network. The extracted features can be called feature layers, which are the feature sets of the input images. In the backbone part, we obtain three feature layers for the next step of network construction. FPN is the enhanced feature extraction network of YOLOv7. The three effective feature layers obtained in the backbone part are feature fused, where the purpose of feature fusion is to combine feature information from different scales. In the FPN part, the three feature layers are further extracted for features. YOLO Head is the classifier and regressor of YOLOv7.

## 3. Experimental setup, simulation and materials

### 3.1. Materials

There are three epoxy-carbon prepreg plates with different types of defects. The three samples were made of epoxy-carbon prepreg (HexPly 914C-T300H (6 K)-6-34%). The plates were obtained with a 24 plies quasi-isotropic lay-up ( $0/+45^\circ/90^\circ/-45^\circ$ ) s. Sample 1 was subjected to impact loading, and the dimension of sample 1 is 100 x 170 x 3.27 mm. The impactor is a 16 mm diameter hemisphere, which falls freely to impact the plate. There are multiple inserts with 10 x 10 mm of length and width and different heights in sample 2, and the dimension of sample 2 is 580 x 280 x 3.4 mm. There are multiple inserts with 6 x 6 mm of length and width and different heights in sample 3, and the dimension of sample 3 is 280 x 220 x 3.5 mm. The schematic image of the samples is shown in Fig. 2.

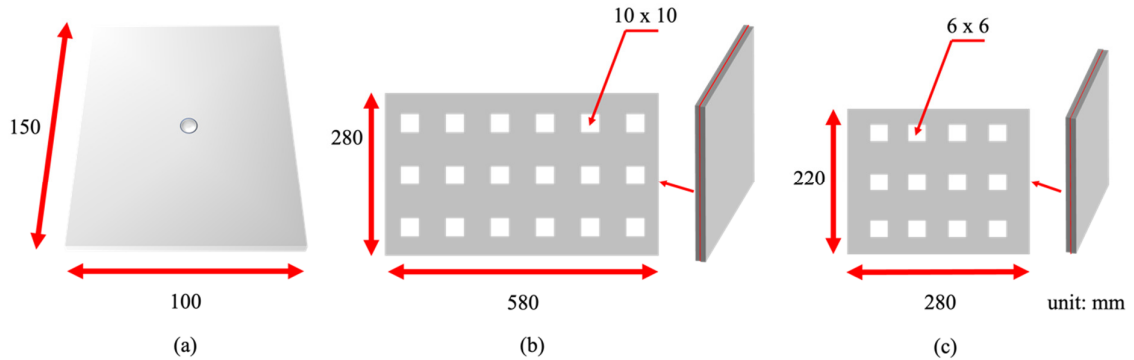
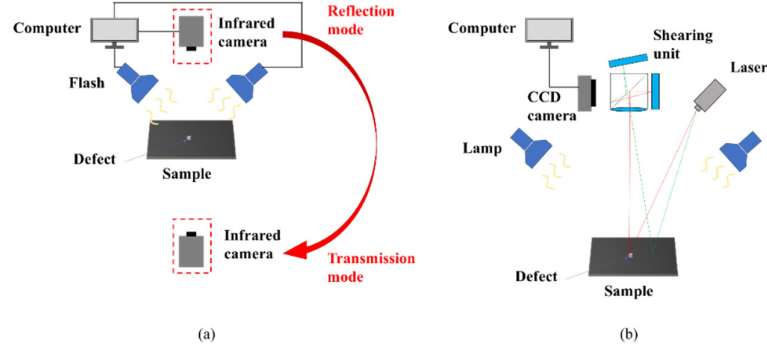


Fig. 1. The schematic image of different samples: (a) sample 1; (b) sample 2; (c) sample 3

### 3.2. Experimental setup

Infrared thermography (IRT) and shearography were used to detect the defects in the Epoxy-carbon prepreg plates. The inspection by active infrared thermography consists of using a heat source that sends a thermal wave that penetrates an object being inspected. This thermal wave will interact with any discontinuity present in the object. The thermal pulse is disturbed at each interface and is captured in the form of an image on the surface of the object, using an infrared camera which sends a real time image to a display screen for interpretation. The schematic image of IRT is shown in Fig. 2(a). Four lamps with the power of 1000 W and an infrared camera (FLIR T450, band 8-12 micrometers, thermal resolution 30 mK) are utilized. In addition, the reflection mode and transmission mode of infrared thermography were performed to detect the defects in each sample. The inspection by shearography consists of using a heat source or another mechanical solicitation that sends a wave or vibration which penetrates an object being inspected. This wave will interact with any discontinuity present in the object which creates a discontinuity in the fringes. The schematic image of shearography is shown in Fig. 2(b). The SLM laser (Power 200 mW, wavelength 532 nm) was used to illuminate the sample surface. The CMOS sensor of the camera (GiGE camera, 2464 x 2056 pixels) is at a distance of 1 m from the sample. The resolution of the thermal sensor is 640 x 480 pixels, and the resolution of the thermal sensor is 55 mK. The front side and back side of each sample were tested by shearography.



**Fig. 2.** Schematic image of infrared thermography and shearography: (a) reflection mode and transmission mode of infrared thermography; (b) shearography

### 3.3. Datasets acquisition

The infrared thermography and shearography were simulated based on Comsol software for dataset preparation. For infrared thermography, heat transfer module in solids was used. The upper surface of sample was subjected by the heat flux load, which the power of the load is  $2 \times 10^4 \text{ W/m}^2$ , and the heating time is 0.01 s. The rest of surfaces were subjected by the convective load, which the film coefficient is  $10 \text{ W/(m}^2\text{C)}$ . The experimental results can be used for training, as shown in Fig. 3. For shearography, the structure mechanics module was used. The four sides of sample were fixed, and the upper surface of sample was subjected by the constant temperature load, which the power of the load is  $100 \text{ }^\circ\text{C}$ . When the deformation distribution  $\Delta(x, y)$  is obtained, a phase map  $\Delta(x, y)$  can be calculated according to the principle of digital shearography. Suppose the shearing direction is along  $k = (\cos\alpha, \sin\alpha)^T$ , the phase difference (phase map)  $\Delta(x, y)$  between before and after loading is denoted as

$$\begin{aligned} \Delta &= \frac{4\pi\delta_k}{\lambda} \frac{\partial\omega}{\partial k} \\ &= \frac{4\pi\delta_k}{\lambda} \left( \frac{\partial\omega}{\partial x} \cos\alpha + \frac{\partial\omega}{\partial y} \sin\alpha \right) \end{aligned} \quad (1)$$

where  $\lambda$  is the laser wavelength and  $\delta_k$  is the shearing value in the  $k$  direction. With different settings in shearing value and shearing direction of just one simulated deformation distribution, amounts of simulated phase maps will be calculated [17].

The samples are divided into three types. The first type is the plate with blind holes, the second type is the plate with inserts, and the last type is the plate with impact damage. The first two samples are modeled by Boolean operations. For the plate with impact damage, the solid mechanics module was used. The large plastic strains model and isotropic hardening model are chosen. The friction coefficient between the rigid ball and the plate is 0.3, and four sides of the plate are fixed. The model after the impact was exported for the detection of infrared thermography and shearography.

In particular, a data augmentation method is used to improve the detection ability of network [18]. MixUp augments the training set by linearly interpolating a random pair of examples and their corresponding labels selected in a minibatch through permutation

$$\begin{aligned} \tilde{x}_i &= \lambda x_i + (1-\lambda)x_j \\ \tilde{y}_i &= \lambda y_i + (1-\lambda)y_j \end{aligned} \quad (2)$$

where  $(x_i, y_i)$  and  $(x_j, y_j)$  are two data-target samples randomly drawn from the training set, and  $\lambda \in [0, 1]$  is the interpolation weighing coefficient. Then, the objective of a supervised problem becomes minimizing the empirical risk over the MixUp-generated samples. The images after MixUp augmentation processing are shown in Fig. 3.

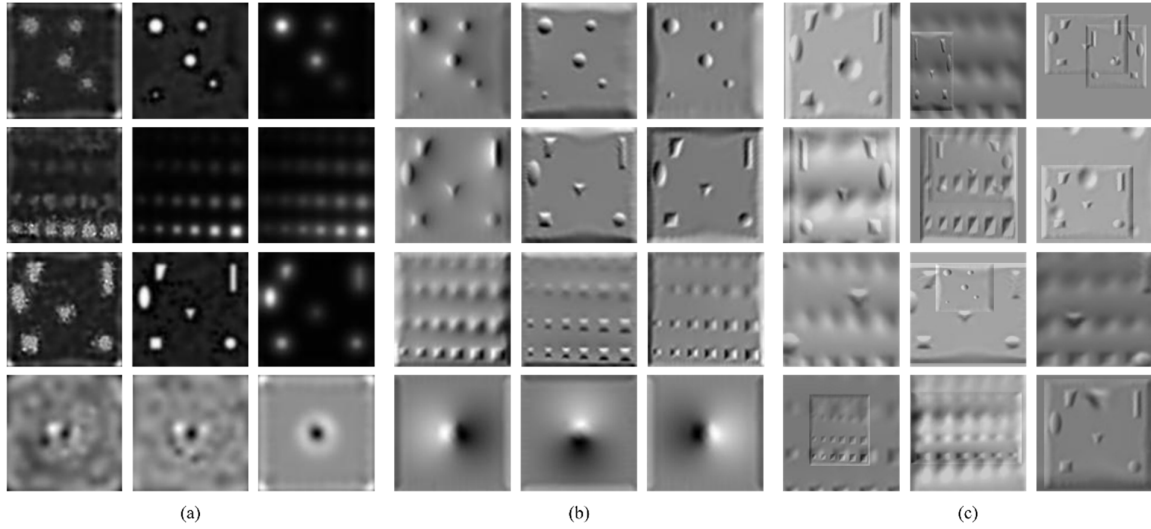


**Fig. 3.** Datasets for deep learning: (a) dataset from infrared thermography; (b) dataset from shearography; (c) dataset from MixUp technique

#### 4. Results and Analysis

In this work, to reduce the image noise and enhance the image contrast, principal component analysis was used for image processing, as shown in Fig. 4. For sample 1 in transmission mode, the damaged area is an elliptical area with vertical areas at both ends, instead of only a circular area, as shown in Fig. 4(c) and (d). The results illustrate that infrared thermography has a higher detection ability than shearography for impact damage. For sample 2 in reflection mode, the upper defects can be detected by infrared thermography, but the bottom defects cannot be detected by IRT. The results of shearography are opposite to that of IRT. The bottom defects can be detected by shearography. For sample 2 in transmission mode, the IRT has a higher detection ability than shearography. The middle defects can be detected by IRT, but it is difficult to detect by shearography. For the experimental results of sample 3, it is possible to find that the left defects can be detected by IRT, and the right defects can be detected by shearography, as shown in Fig. 4(i)-(l). In conclusion, IRT and shearography are complementary. This provides the basis for the convergence of the two technologies.

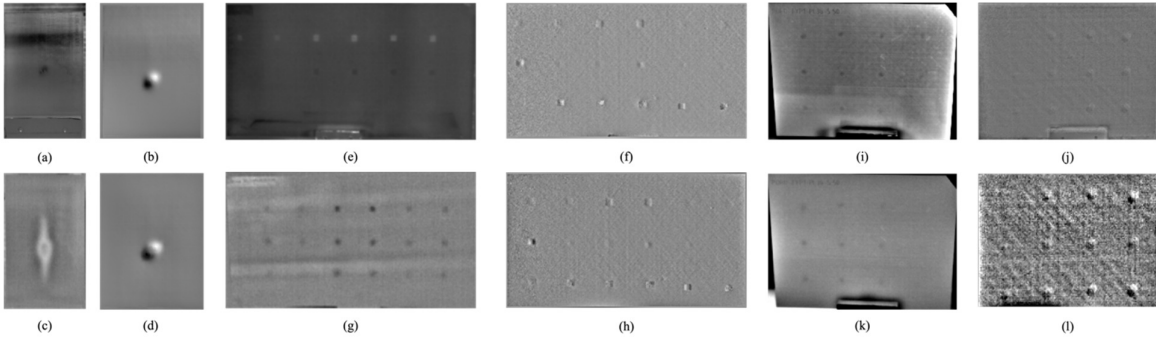


**Fig. 4.** Experimental results after image processing: (a), (c), (e), (g), (i), (k) are the raw images of infrared thermography; (b), (d), (f), (h), (j), (l) are the raw images of shearography; (a) and (b) are the results for sample 1 using reflection mode; (c) and (d) are results for sample 1 using transmission mode; (e) and (f) are the results for sample 2 using reflection mode; (g) and (h) are the results for sample 2 using transmission mode; (i) and (j) are results for sample 3 using reflection mode; (k) and (l) are results for sample 3 using transmission mode

##### 4.1. Data fusion results

As mentioned before, the experimental results of infrared thermography are complementary to that of shearography. In this section, different data fusion techniques were used to further detect the defects based on IRT and shearography.

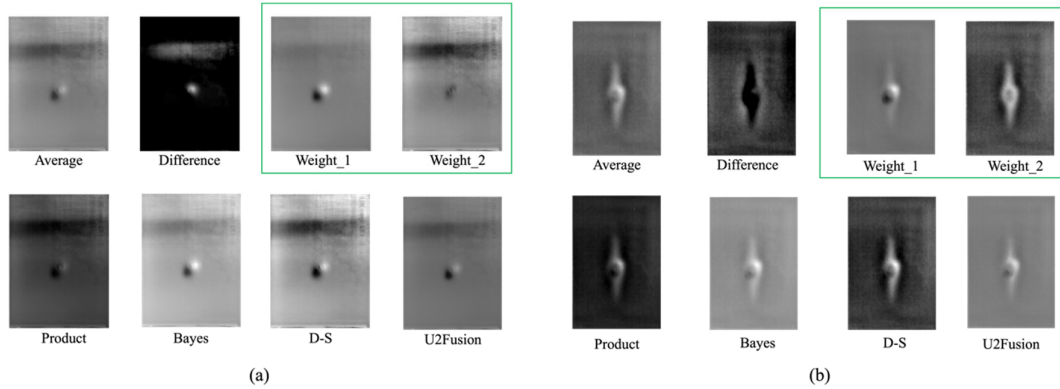


**Fig. 5.** Data fusion results for sample 1: (a) reflection mode; (b) transmission mode; *Weight\_1* denotes weighted average method of  $(5*SH+IR)/6$ ; *Weight\_2* denotes weighted average method of  $(SH+5*IR)/6$ ; *Bayes* denotes Bayesian analysis method; *D-S* denotes Dempster-Shafer method

For sample 1 in reflection mode, it is possible to find that the image quality based on the fusion techniques of “Difference” and “Weight\_2” is poor, as shown in Fig. 5(a). The color of the image processed by the “Difference” method is dark, which leads to the reduction of damage information. The images processed by the “Weight\_2” method either lose the damage information of IRT or shearography. The “D-S” method enhances the image contrast and retains most of the damage information from IRT and shearography. Furthermore, the image processed by the “Product” method has lower contrast than the images processed by the “Average”, “Weight\_1” “U2Fusion” and “Bayes” methods.

For sample 2 in reflection mode and transmission, the detection ability based on the data fusion technique obviously increases, as shown in Fig. 6. Compared with the PCA images, the images after data fusion processing can detect more defects. Furthermore, the image contrast extremely increases. For instance, the image processed by the “D-S” method, “Weight\_1” and “Product” methods in transmission mode have high contrast and low noise. However, the images processed by the “Difference” method lose many defects information both in reflection mode and transmission mode. The image processed by the “U2Fusion” method has low image contrast.

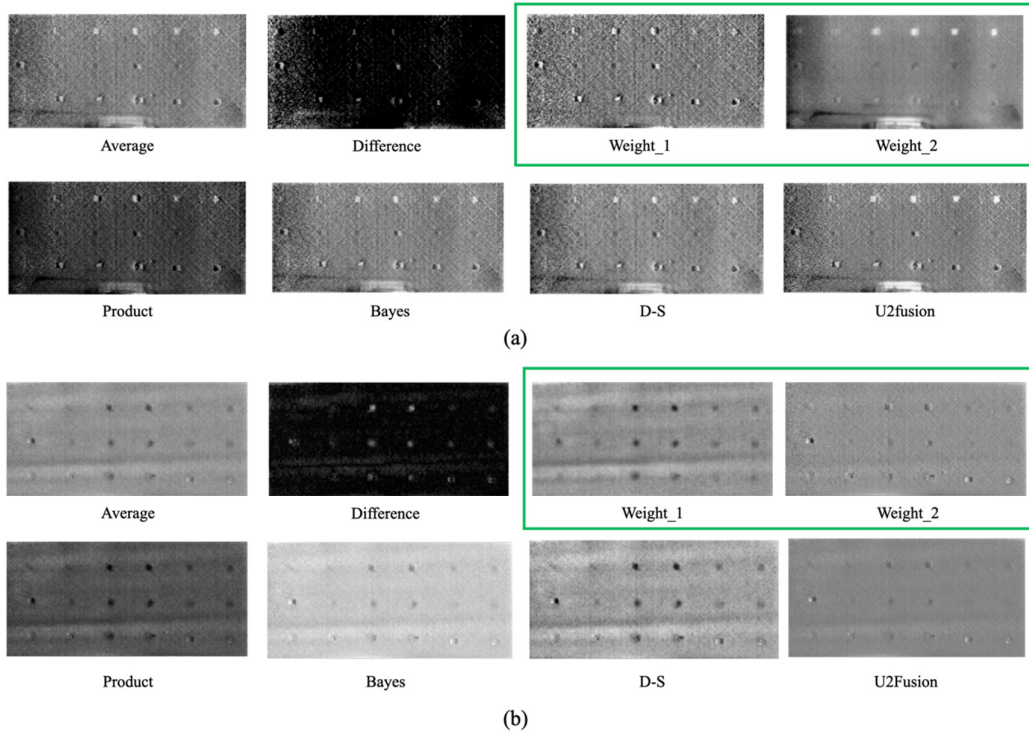


**Fig. 6.** Data fusion results for sample 2: (a) reflection mode; (b) transmission mode; *Weight\_1* denotes weighted average method of  $(5*SH+IR)/6$ ; *Weight\_2* denotes weighted average method of  $(SH+5*IR)/6$ ; *Bayes* denotes Bayesian analysis method; *D-S* denotes Dempster-Shafer method

For sample 3 in reflection mode, the images processed by the “D-S” and “Product” methods have high contrast, as shown in Fig. 7(a). It is difficult to distinguish the defective areas and the non-defective areas in the image processed by the “Difference” method. The images processed by the “Average”, “Weight\_1”, “Weight\_2”, and “U2fusion” methods have low contrast, which means that the defects are hard to be observed. For sample 3 in transmission mode, the image processed by the “Weight\_2” method can detect all defects, as shown in Fig. 7(b). The image processed by the “Product” method has low contrast. It is difficult to detect the left defects in the images processed by “Average”, “Weight\_1”, “Bayes”, “D-S”, and “U2Fusion” methods.

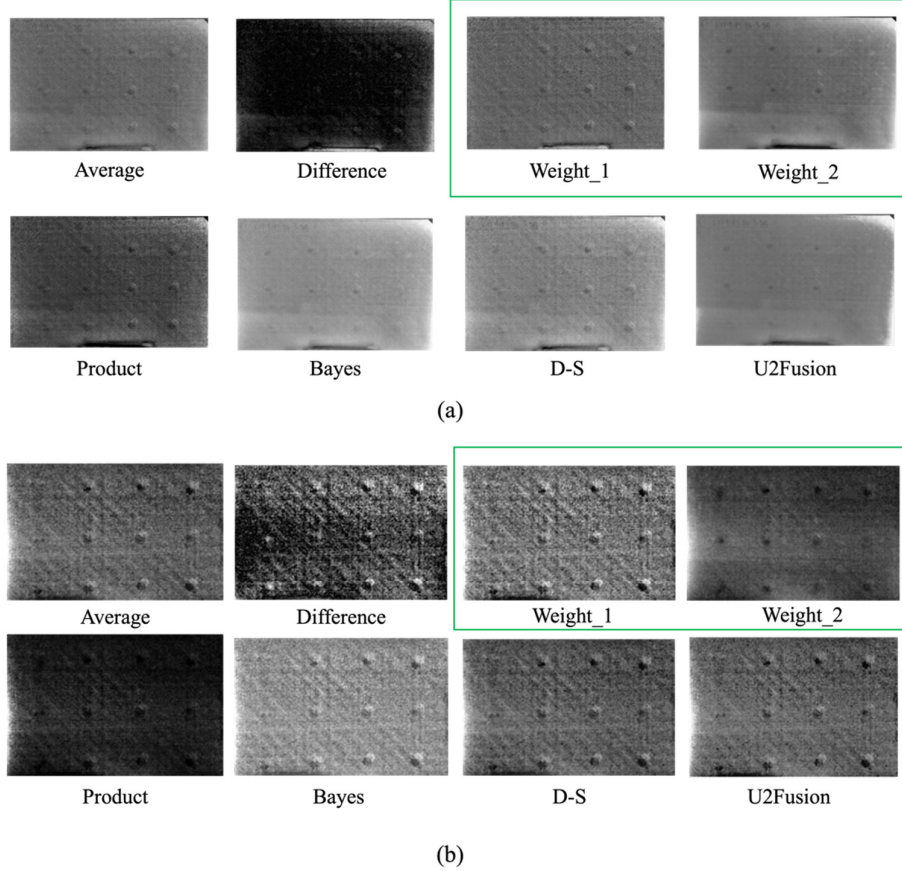


**Fig. 7.** Data fusion results for sample 3: (a) reflection mode; (b) transmission mode; Weigh\_1 denotes weighted average method of  $(5*SH+IR)/6$ ; Weigh\_2 denotes weighted average method of  $(SH+5*IR)/6$ ; Bayes denotes Bayesian analysis method; D-S denotes Dempster-Shafer method

To quantitatively analyze the image quality based on different data fusion methods, Peak-Signal to Noise Ratio (PSNR) is used herein instead of Signal to Noise Ratio (SNR). Because the pixel values of the defective area in shearography are either higher or lower than that of the non-defective area. The SNR method is to calculate the average values of defective areas for the evaluation of image quality. In this case, the pixel values of the defective area are neutralized, and it is difficult to be distinguished from the non-defective area. The PSNR is expressed as follows:

$$PSNR = 10 \log_{10} \frac{255^2}{MN \sum_{i=1}^M \sum_{j=1}^N |R(i, j) - F(i, j)|^2} \quad (3)$$

where  $F$  represents the intensity of defective areas,  $R$  represents the intensity of sound areas, and  $M, N$  are the image size. It is noted that the lower the PSNR value, the larger the image contrast. The PSNR values of the images processed by different data fusion techniques are shown in Fig. 8. It is obvious to find that the “D-S” method has the best effect on image contrast. The effect of the “Bayes” method is second to the “D-S” method. Although the “U2Fusion” method is a novel unsupervised learning method for data fusion of infrared images and visible images, the results of the “U2Fusion” method are not better than the classic methods. Among classical methods, the “weight\_1” method has the best effect on image contrast.

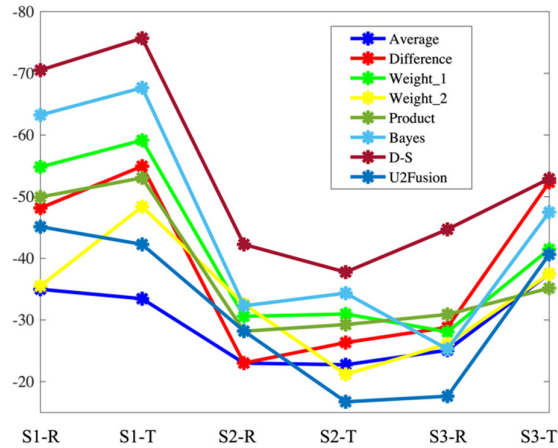


**Fig. 8.** The PSNR values of the images processed by different data fusion techniques: S1-R denotes the results of sample 1 in reflection mode; S1-T denotes the results of sample 1 in transmission mode; S2-R denotes results of sample 2 in reflection mode; S2-T denotes the results of sample 2 in transmission mode; S3-R denotes the results of sample 3 in reflection mode; S3-T denotes the results of sample 3 in transmission mode

#### 4.2. Automatic defect detection in data fusion view

In this section, the object detector algorithm YOLOv7 is used to detect subsurface defects. The datasets described in section 3.3 are used. The results of D-S method are shown as in Fig. 9.

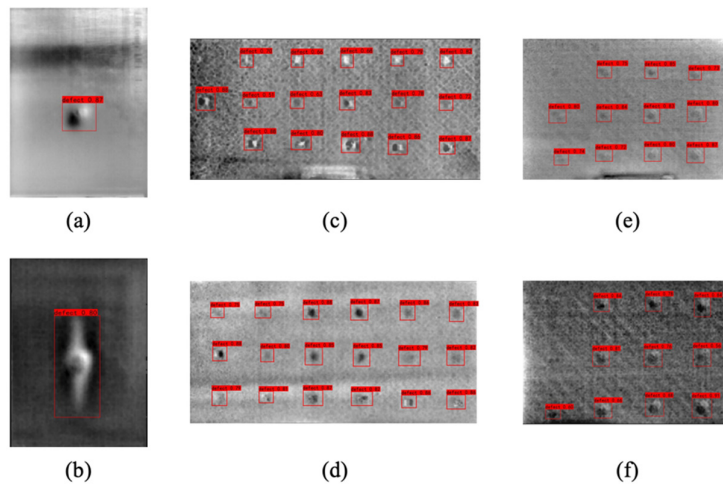


**Fig. 9.** The automatic detection for D-S method: (a) and (b) denote sample 1; (c) and (d) denote sample 2; (e) and (f) denote sample 3

The performance of different data fusion techniques is shown in Table 2. The results show that the “D-S” method has the best detection capacity among all data fusion techniques, while the “Difference” method is the worst data fusion technique. In summary, the ranking of detection ability is D-S > Average > Product » Weight\_2 » Weight\_1 > Bayes > U2Fusion > Difference.

**Table 2.** The performance of different data fusion techniques

Method	Sample 1		Sample 2		Sample 3	
	RM	TM	RM	TM	RM	TM
	D/F	D/F	D/F	D/F	D/F	D/F
Average	1/0	1/0	14/0	18/0	11/0	10/0
Difference	1/0	1/0	9/0	14/0	3/0	7/1
Weight_1	1/0	1/0	15/0	16/0	11/0	11/1
Weight_2	1/0	1/0	14/0	17/0	10/1	10/0
Product	1/0	1/0	15/0	18/0	11/1	9/0
Bayes	1/0	1/0	14/0	17/0	10/1	9/0
D-S	1/0	1/0	16/0	18/0	11/0	10/0
U2Fusion	1/0	1/0	15/0	15/0	10/3	11/2

RM denotes reflection mode, TM denotes transmission mode, D/F denotes detected defects / misdetected defects.

## 5. Conclusion

In this work, infrared thermography and shearography technologies are used for the defect detection of epoxy-carbon prepreg laminates. The principal component analysis is performed as an image processing method to enhance the image contrast and reduce the image noise. The results show that these two technologies are complementary. To improve the detection ability, data fusion techniques are involved around the results of these two technologies. Different data fusion techniques such as “average”, “difference”, “weighed average”, “product”, “Bayes”, and “Dempster-Shafer” methods are applied to the PCA results of these two sensors. In addition, a novel unsupervised network named U2Fusion is also used for the data fusion of PCA results. The PSNR is used to evaluate the detection ability of different data fusion results. Finally, an automated defect detection method named YOLOv7 is used to detect the defects in the data fusion view. To improve the detection ability of YOLOv7, a data augmentation method named MixUp is used to construct the datasets obtained from the simulation. The experimental results show the excellent detection ability of the proposed method. Furthermore, both PSNR and YOLOv7 methods show that the “Dempster-Shafer” method has the best detection ability among all used data fusion methods. Looking forward, the development of an automatic system for identifying defects in curing process based on the data fusion of infrared thermography and shearography shall be undertaken for industrial applications.

## Acknowledgments

This work was supported by the Natural Sciences and Engineering Research Council (NSERC) Canada through the Discovery and CREATE ‘oN DuTy!’ program as well as the Canada Research Chair in Multipolar Infrared Vision (MiViM).

We acknowledge the contribution of Ministère des Relations internationales et de la Francophonie of Quebec and Wallonia government in the framework of the Quebec/Wallonia-Brussels scientific collaboration, project number 12.801.

## REFERENCES

- [1] R.S. Dave, A.C. Loos, Processing of Composites, Hanser Publishers, 2000.
- [2] J. Hu, H. Zhang, S. Sfarra, C. Santulli, G. Tian, X. Maldague, Novel infrared-terahertz fusion 3D non-invasive imaging of plant fibre-reinforced polymer composites, Compos. Sci. Technol. 2022;226:109526.

- [3] H. Zhang, P. Verberne, S.A. Meguid, C.I. Castanedo, X.P.V. Maldague, Autonomous high resolution inspection of kiss-bonds skins of carbon nanotube reinforced nanocomposites using novel dynamic line-scan thermography approach, *Compos. Sci. Technol.* 2020;192:108111.
- [4] H. Zhang, L. Yu, U. Hassler, H. Fernandes, M. Genest, F. Robitaille, S. Joncas, W. Holub, Y. Sheng, X. Maldague, An experimental and analytical study of micro-laser line thermography on micro-sized flaws in stitched carbon fiber reinforced polymer composites, *Compos. Sci. Technol.* 2016;126:17-26.
- [5] H. Fernandes, H. Zhang, C.I. Castanedo, X. Maldague, Fiber orientation assessment on randomly-oriented strand composites by means of infrared thermography, *Compos. Sci. Technol.* 2015;121:25-33.
- [6] H. Zhang, F. Robitaille, C.U. Grosse, C.I. Castanedo, J. O. Martins, S. Sfarra, X.P.V. Maldague, Optical excitation thermography for twill/plain weaves and stitched fabric dry carbon fibre preform inspection, *Compos. Part A-Appl. S.* 2018;107:282-293.
- [7] N. Tao, A.G. Anisimov, R.M. Groves, FEM-assisted shearography with spatially modulated heating for non-destructive testing of thick composites with deep defects, *Compos. Struct.* 2022;297:115980.
- [8] L. Zhang, F.S. Cui, B. Mutiargo, L. Ke, Z.W. Tham, Y.F. Chen, C.Y. Tan, Defect imaging in carbon fiber composites by acoustic shearography, *Compos. Sci. Technol.* 2022;223:108417.
- [9] L.S. Liu, C.J. Guo, Y.X. Xiang, Y.X. Tu, L.M. Wang, F.Z. Xuan, Photothermal Radar Shearography: A Novel Transient-Based Speckle Pattern Interferometry for Depth-Tomographic Inspection, *IEEE T. Ind. Inform.* 2022;18:4352-4360.
- [10] S.L. Wu, Y.F. Yao, B. Wang, Y.H. Wang, F.L. Yang, A Synchronous Measurement System for the First Derivative Out-of-Plane Deformation of Double Ends, *IEEE T. Instrum. Meas.* 2022;71:7004308.
- [11] B. Yilmaz, A. Ba, E. Jasiuniene, H.K. Bui, G. Berthiau, Evaluation of Bonding Quality with Advanced Nondestructive Testing (NDT) and Data Fusion, *Sensors* 2020;20:5127.
- [12] C. Völker, P. Shokouhi, Multi sensor data fusion approach for automatic honeycomb detection in concrete, *NDT & E Int.* 2015;71:54-60.
- [13] X.E. Gros, Z. Liu, K. Tsukada, K. Hanasaki, Experimenting with Pixel-Level NDT Data Fusion Techniques, *IEEE T. Instrum.* 2000;49:1083-1090.
- [14] X.E. Gros, J. Bousigue, K. Takahashi, NDT data fusion at pixel level, *NDT & E Int.* 1999;32:283-292.
- [15] H. Xu, J. Ma, J. Jiang, X. Guo, H. Ling, U2Fusion: A Unified Unsupervised Image Fusion Network, *IEEE T. Pattern. Anal.* 2022;44:502-518.
- [16] C.Y. Wang, A. Bochkovskiy, H.Y.M. Liao, YOLOv7: Trainable bag-of-freebies sets new state-of-the-art for real-time object detectors, *arXiv preprint* 2022;2207:02696.
- [17] W. Li, D. Wang, S. Wu, Simulation Dataset Preparation and Hybrid Training for Deep Learning in Defect Detection Using Digital Shearography, *Appl. Sci-Basel* 2022;12:6931.
- [18] H. Zhang, M. Cisse, Y.N. Dauphin, D. L. Paz, mixup: BEYOND EMPIRICAL RISK MINIZATION, *arXiv preprint* 2017;1710:09412.